Acta Crystallographica Section D
**Biological Crystallography**
ISSN 0907-4449

# Expression, purification and crystallization of a BH domain from the GTPase regulatory protein associated with focal adhesion kinase

**P. J. Sheffield,[a] U. Derewenda,[a] J. Taylor,[b] T. J. Parsons[b] and Z. S. Derewenda[a]***

[a]Department of Physiology, University of Virginia, Charlottesville, VA 22908, USA, and [b]Department of Microbiology, University of Virginia, Charlottesville, VA 22908, USA

Correspondence e-mail: zsd4n@virginia.edu

Received 15 April 1998
Accepted 1 July 1998

Signaling by small GTPases is down-regulated by GTPase activating proteins (GAPs) which enhance the rate of GTP hydrolysis. The activity of GAPs specific for Rho GTPases resides in the BH domain, many homologues of which are found in any mammalian genome. One of them was identified in the GTPase regulator associated with focal-adhesion kinase (GRAF). It shares approximately 20% sequence identity with p50RhoGAP. This GAP activates RhoA and Cdc42Hs, but not Rac. In order to dissect the molecular basis of this specificity, a 231-residue-long fragment corresponding to the BH domain of GRAF has been expressed, purified and crystallized. Trigonal crystals, of space group $P3_121$ or $P3_221$, with unit-cell dimensions $a = b = 63.5$, $c = 90.38$ Å were grown from solutions of PEG 6000. Data to 2.15 Å were collected from a flash-frozen sample on an R-AXIS IV imaging-plate detector mounted on a rotating-anode X-ray generator.

## 1. Introduction

The Rho family of small GTPases (Rho, Rac and Cdc42) plays a crucial role in signal transduction by causing rearrangement of the actin cytoskeleton (stress-fiber formation) and the association of focal-adhesion complexes (Hall, 1990; Ridley *et al.*, 1992; Ridley & Hall, 1992; Ridley, 1994). These proteins function as molecular switches, 'on' when bound to GTP and 'off' when bound to GDP. The cyclic turnover of GTP by all small GTPases is regulated by several distinct families of accessory proteins, such as nucleotide-exchange factors (GEFs) which promote GDP–GTP exchange (Bourne *et al.*, 1990, 1991), nucleotide-dissociation inhibitors (GDIs), which inhibit GDP–GTP exchange (Lancaster *et al.*, 1994), and GTPase-activating proteins (GAPs), which promote GTP hydrolysis (Boguski & McCormick, 1993; Diekmann *et al.*, 1991; Hall, 1990). Rho-specific GAPs are typically multidomain proteins with the GTPase activating activity residing in a specific domain, known as the breakpoint cluster homology (BH) domain. To date, two BH-domain structures have been solved: the BH domain from phosphoinositide 3-kinase p85$\alpha$ subunit (Musacchio *et al.*, 1996) and from p50RhoGAP (Barrett *et al.*, 1997). Although the sequence homology between the p85$\alpha$ subunit and p50RhoGAP is low, at approximately 20%, they share a common tertiary fold consisting of eight $\alpha$-helices (Barrett *et al.*, 1997; Musacchio *et al.*, 1996), distinct from the GTPase-activating domain of p120RasGAP (Scheffzek *et al.*, 1996). The biochemical role of GAPs is to down-regulate the biological activity of GTPases by binding to the GTP-bound 'on' form and increasing the rate of GTP hydrolysis, thereby returning the protein to the GDP-bound 'off' form. The recently reported structures of the p50RhoGAP BH domain in complexes with Cdc42Hs and RhoA–$AlF_4^-$ (Rittinger, Walker, Eccleston, Nurmahomed *et al.*, 1997; Rittinger, Walker, Eccleston, Smerton *et al.*, 1997) yielded significant insight into the molecular mechanisms involved in the process. Two residues, Arg85 and Asn194, play key roles, with the former involved directly in catalysis *via* the so-called arginine-finger mechanism also found in p120RasGAP (Scheffzek *et al.*, 1997). However, the molecular basis of specificity of GAPs is much less well understood.

BH domains occur in a range of multi-domain proteins which have been shown to contain other regions that are involved in other protein–protein interactions (Lancaster *et al.*, 1994; Chuang *et al.*, 1995; Trahey *et al.*, 1988; Vogel *et al.*, 1988), *e.g.* SH3 domains and PH (pleckstrin homology) domains. These domains offer a targeting mechanism by which signals mediated by GTPases are transferred to specific downstream effectors, *e.g.* Rho-sensitive protein kinases.

A partial cDNA clone, encoding for a GTPase regulator associated with focal-adhesion kinase GRAF (GTPase regulator associated with FAK), was recently isolated from chicken-embryo cells (Hildebrand *et al.*, 1996). Although the extreme 5′ end of the clone has not been identified, it is clear that the carboxyl end of the gene product contains a BH domain linked to an SH3 domain. The protein has been shown to bind to

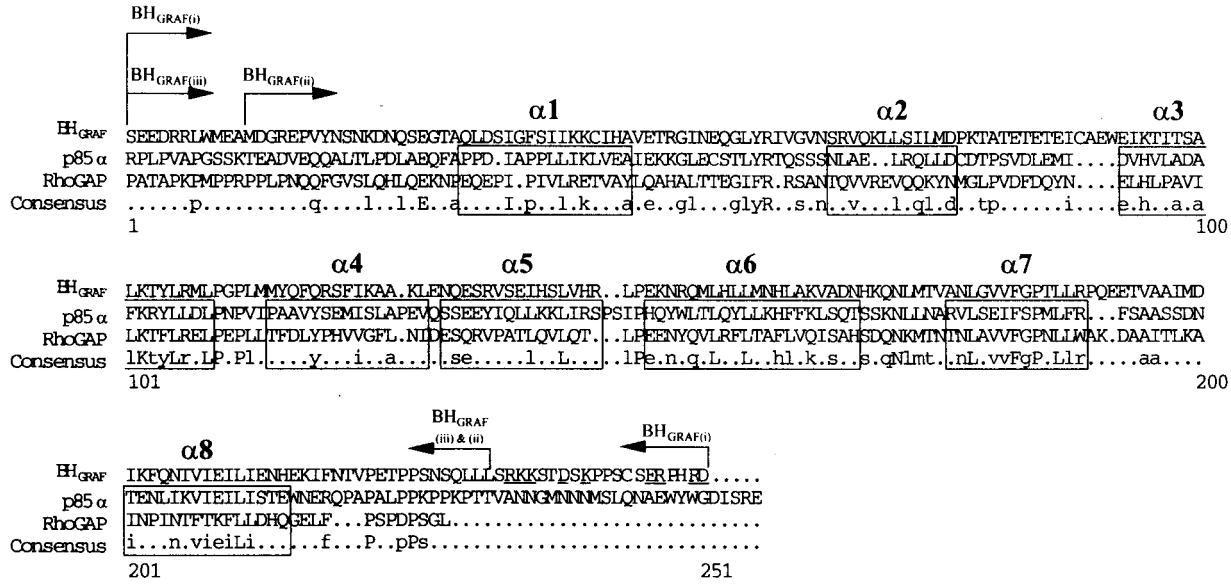


**Figure 1**
Protein-sequence alignment of $BH_{GRAF}$, p85$\alpha$ subunit and RhoGAP showing position of the helices in boxes. Full length $BH_{GRAF}$ sequence corresponds to $BH_{GRAF(i)}$. The stop codon was introduced after the Leu triplet at position 231. $BH_{GRAF(ii)}$ extends from Met12 to Leu231 and $BH_{GRAF(iii)}$ from Ser1 to Leu231.

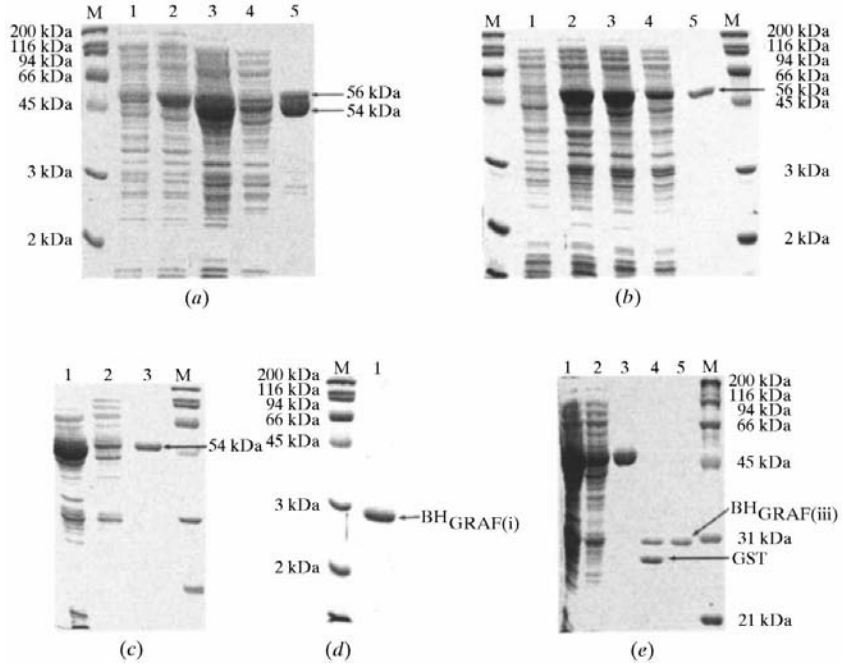


**Figure 2**
SDS gels of $BH_{GRAF}$ expression and purification. (*a*) $BH_{GRAF(i)}$ expression in XL1Blue; M = markers, lane 1, uninduced; lane 2, induced; lane 3, soluble fraction; lane 4, glutathione Sepharose column flow through; lane 5, elution of 56 kDa and 54 kDa GST-BHs. (*b*) $BH_{GRAF(i)}$ expression in BL21; lane 1, total cell protein uninduced; lane 2, total cell protein induced; lane 3, soluble fraction; lane 4, glutathione Sepharose column flow through; lane 5, elution of 56 kDa GST-BH. (*c*) $BH_{GRAF(i)}$ expression in XL1Blue including 2 h incubation after cell lysis to allow proteolysis; lane 1, soluble fraction; lane 2, glutathione Sepharose column flow through; lane 3, $BH_{GRAF(i)}$ elution of 54 kDa GST-BH. (*d*) Pure $BH_{GRAF(i)}$ after size exclusion. (*e*) $BH_{GRAF(iii)}$ expression in XL1Blue; lane 1, induced; lane 2, soluble fraction; lane 3, elution of 54 kDa GST-$BH_{GRAF}$; lane 4, post-thrombin digestion; lane 5, pure $BH_{GRAF(iii)}$.

Cdc42Hs and RhoA *via* the BH domain and to the proline-rich C-terminus of focal-adhesion kinase *via* the SH3 domain (Hildebrand *et al.*, 1996). Initially, a 256-residue fragment containing the BH domain was overexpressed in *Escherichia coli* as a GST fusion. However, in order to obtain a protein that purified and crystallized well, the cDNA had to undergo several alterations.

## 2. Materials and methods

### 2.1. Bacteria, plasmids and media

DNA manipulations and protein expression were performed in *Escherichia coli* strain XL1Blue {*recA1 endA1 gyrA96 thi-1 hsdR17 supE44 relA1 lac* [*F′ proAB lacI*$^q$*ZΔM15 Tn10* (*Tet*$^R$)]$^c$} (Stratagene). The glutathione-S-transferase expression vector, pGEX4T1, was obtained from Pharmacia. A derivative of pGEX4T1, pGEX-Universal1, was created by replacement of the thrombin cleavage site with a tobacco etch virus (TEV) protease cleavage site. Luria broth (LB) was used throughout as the standard growth media for both plasmid manipulation and protein expression.

### 2.2. Manipulation of *BH$_{GRAF}$* gene

The *BH$_{GRAF}$* gene was subcloned into pGEX4T1 and the SH3 domain was removed by deletion of the 3′ end of the *BH$_{GRAF}$* gene, resulting in pGEX4T1–$BH_{GRAF(i)}$. The polymerase chain reaction (PCR) was used to create $BH_{GRAF(ii)}$ by the introduction of a *Sal*I site and a stop codon after Leu231 and an *Nco*I site over Met12 (Fig. 1). The PCR fragment was subcloned into pGEX-Universal1 by use of the *Nco*I and *Sal*I sites. The integrity of the pGEXUni1–$BH_{GRAF(ii)}$ construct was confirmed by DNA sequencing. $BH_{GRAF(iii)}$ was created by exchanging the C-terminal region of $BH_{GRAF(i)}$ with the C-terminal region of $BH_{GRAF(ii)}$. The C-terminus of $BH_{GRAF(ii)}$ was isolated from pGEXUni1–$BH_{GRAF(ii)}$ as a *Bam*HI/*Not*I fragment and

subcloned into pGEX4T1–$BH_{GRAF(i)}$ similarly digested.

### 2.3. Expression conditions

Expression of all three versions of the BH domain was performed in 1–4 l cultures of LB and incubated at 310 K until an $OD_{600}$ of 0.4–0.6; expression was induced by the addition of IPTG (to a final concentration of 500 µ*M*). The cultures were grown for a further 16 h at 296 K. Cells were harvested by centrifugation, re-suspended in GST buffer (150 m*M* NaCl, 50 m*M* Tris–HCl, pH 8.5 and 5 m*M* EDTA; 5 ml per gram of cell pellet), lysed by sonication and the soluble protein fraction recovered by centrifugation. Cell pellets containing $BH_{GRAF(i)}$ were incubated at 296 K for 3 h after sonication to allow $BH_{GRAF(i)}$ to be fully proteolyzed.

### 2.4. GST affinity purification

GST fusion proteins were isolated by binding to glutathione Sepharose columns (Pharmacia). The soluble protein fraction was allowed to bind to the column for 2 h at room temperature before being washed with 2 l of GST buffer at 277 K. Fusion protein was eluted in 20 ml of GST buffer containing 10 m*M* reduced glutathione pH 8.5. The GST tag was removed by incubating with either thrombin (Sigma) or rTEV (Gibco-BRL) for 36 h at 303 K. The cleavage products were dialyzed against 2 l of GST buffer to remove the glutathione before being rebound to a glutathione Sepharose column to remove the contaminating GST protein. This procedure removed over 90% of the GST protein; the residual GST was removed by size-exclusion chromatography (Superdex 75 column; Pharmacia). The different versions of the BH domains were dialyzed against 20 m*M* Tris–HCl pH 8.6 for use in crystallization trials.

### 2.5. Purification of Cdc42Hs

*E. coli* containing the pGEX2T–Cdc42Hs expression vector (supplied by Alan Hall) were grown to log phase and protein expression induced with 0.1 m*M* IPTG for 3 h. Bacteria were pelleted, resuspended in lysis buffer (50 m*M* Tris pH 7.5, 50 m*M* NaCl, 5 m*M* $MgCl_2$, 1 m*M* DTT and 1 mg $ml^{-1}$ lysozyme), sonicated and pelleted. The supernatants were bound to glutathione Sepharose beads at 277 K for 1 h. GST–Cdc42Hs was cleaved with thrombin (3 units per 2 ml of beads) for 12–16 h at 277 K in a buffer consisting of 50 m*M* Tris pH 8.0, 150 m*M* NaCl, 5 m*M* $MgCl_2$, 2.5 m*M* $CaCl_2$ and 1 m*M* DTT. After cleavage, the thrombin was removed using *p*-aminobenzamidine beads (Sigma). Purified Cdc42Hs was then dialysed against 150 m*M* Tris pH 8.0, 150 m*M* NaCl, 5 m*M* $MgCl_2$ and 1 m*M* DTT, concentrated to 1 mg $ml^{-1}$ and stored at 203 K until use.

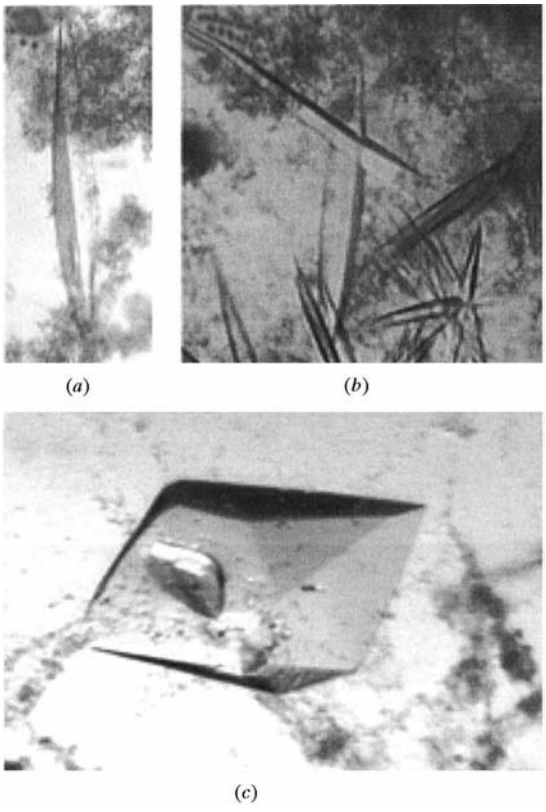


**Figure 3**
$BH_{GRAF}$ crystals. (*a*) and (*b*) Crystals of similar morphology were obtained for both $BH_{GRAF(i)}$ and $BH_{GRAF(iii)}$ from 17% PEG 4000, 100 m*M* Tris–HCl, pH 8.5, 200 m*M* lithium sulfate. (*c*) Trigonal $BH_{GRAF(iii)}$ crystals were obtained from 23% PEG 6000, 100 m*M* Na HEPES, pH 7.0.

### 2.6. BH activity assay

Cdc42Hs (1 µg) was loaded with $\gamma$-$^{32}$P-GTP (20 µCi) for 10 min at 303 K in a total volume of 90 µl of GTPase loading buffer (5 m*M* Tris pH 7.5, 50 m*M* NaCl, 5 m*M* EDTA, 1 mg $ml^{-1}$ BSA and 1 m*M* DTT). The reaction was terminated by the addition of a final concentration of 10 m*M* $MgCl_2$. Purified $BH_{GRAF}$ domains (70–280 ng) or buffer control (50 m*M* Tris pH 8.0) were incubated with 50 ng $\gamma$-$^{32}$P-GTP-loaded Cdc42Hs for 10 min in a buffer containing 50 m*M* Tris pH 7.5, 10 m*M* $MgCl_2$, 1 mg $ml^{-1}$ BSA and 1 m*M* DTT. The reaction was terminated with 500 µl stop buffer (50 m*M* Tris pH 7.5, 10 m*M* $MgCl_2$ and 1 m*M* DTT), filtered through nitrocellulose membranes, washed and counted to determine the amount of $\gamma$-$^{32}$P-GTP remaining bound to Cdc42Hs.

### 2.7. X-ray data collection

Data were collected on an R-AXIS IV dual image-plate detector mounted on an Enraf–Nonius FR 591 rotating-anode generator equipped with dual focusing mirrors (Molecular Structure Corporation). The crystals were flash-frozen at 100 K using the X-Stream device (Molecular Structure Corporation) and PEG 400 as a cryoprotectant. Data were processed with the Linux version of the *HKL* suite (Otwinowski & Minor, 1997) on a Dell PC.

## 3. Results

Expression of pGEX4T1–$BH_{GRAF(i)}$ in *E. coli* strain XL1Blue resulted in the expression and purification of two GST fusion proteins, a 56 kDa protein (expected size) and a 54 kDa protein (Fig. 2*a*). The smaller protein was attributed to an endogenous protease degrading the full length $BH_{GRAF(i)}$ by removing an approximately 2 kDa oligopeptide from the C-terminus. Inclusion of proteinase inhibitors in the lysis buffer had no effect on the degradation event. Expression of $BH_{GRAF(i)}$ was then carried out in *E. coli* strain BL21, an *OmpT* proteinase-deficient strain, resulting in production of only the 56 kDa fusion protein (Fig. 2*b*). However, this protein proved to be unstable and precipitated during purification resulting in low yields (<1 mg $l^{-1}$). It was apparent that the degradation occurred at the C-terminus, as the 56 and 54 kDa proteins were both isolated as N-terminal GST fusions. Examination of the protein sequence revealed a high concentration of charged residues at the C-terminus as well as a free cysteine residue (Fig. 1). Expression was reperformed in XL1Blue and the purification was repeated with a room-temperature incubation step being included to allow the endogenous proteinase to fully degrade the C-terminus of the 56 kDa protein and convert it into the 54 kDa form. The 54 kDa protein showed no precipitation during purification and 5–7 mg $l^{-1}$ of pure $BH_{GRAF(i)}$ was obtained (Figs. 2*c* and 2*d*).

Crystallization experiments were performed by the hanging-drop vapor-diffusion method at 294 K using Linbro 24-

well tissue culture plates. Initial screening was performed using the Hampton Research crystal screen I with a $BH_{GRAF(i)}$ concentration of 3 mg ml$^{-1}$. Micro-crystals formed in 30% PEG 4000, 100 m*M* Tris–HCl pH 8.5, 200 m*M* lithium sulfate and in 200 m*M* ammonium sulfate, 100 m*M* Na HEPES pH 7.5, 2% PEG 400. Further trials were performed around these conditions and better crystals were obtained in 17% PEG 4000, 100 m*M* Tris–HCl pH 8.5, 200 m*M* lithium sulfate with a $BH_{GRAF(i)}$ concentration of 15 mg ml$^{-1}$ (Fig. 3*a*).

To improve crystallization, the DNA was manipulated by the introduction of a stop codon after Leu231. This was performed to eliminate the need for XL1Blue to degrade the C-terminus, as this was not a controlled procedure and, therefore, could lead to sample heterogeneity. In addition to the stop codon, 11 N-terminal residues were removed by the introduction of an *Nco*I site over Met12. Expression of this protein, $BH_{GRAF(ii)}$, resulted in a single 54 kDa GST fusion protein and no degradation was observed. However, the protein proved difficult to purify and precipitated during purification. This suggested that the 11 N-terminus residues were required for protein stability. To correct this, the C-terminus of $BH_{GRAF(i)}$ was replaced by the C-terminus of $BH_{GRAF(ii)}$ to create $BH_{GRAF(iii)}$. Expression of $BH_{GRAF(iii)}$ in XL1Blue resulted in a stable protein product (Fig. 2*e*) which purified well with good yields (7 mg l$^{-1}$).

All three versions of the $BH_{GRAF}$ domain activated the intrinsic GTPase activity of GTP-bound Cdc42Hs in a similar manner (data not shown).

As in the case of $BH_{GRAF(i)}$, two crystal forms were obtained for $BH_{GRAF(iii)}$ (Fig. 3). Crystal screening around the 30% PEG 6000, 100 m*M* Na HEPES, pH 7.0 condition improved the quality of the crystals. The best crystals were obtained from $BH_{GRAF(iii)}$ in 22–24% PEG 6000, 100 m*M* Na HEPES, pH 7.0 at a protein concentration of 8 mg ml$^{-1}$. Crystals appeared after 2 d and grew slowly over two weeks at 294 K. They were trigonal with either a $P3_121$ or $P3_221$ space group. The unit-cell dimensions were $a = b = 63.5$, $c = 90.38$ Å, with one molecule in the asymmetric unit judged by the resulting specific volume of 1.99 Å$^3$ Da$^{-1}$. Diffraction extended to 2.15 Å and native data were collected accordingly. A total of 56545 observations were reduced to 11626 unique reflections, 96.9% complete, with an $R_{merge}$ of 0.056. Molecular-replacement calculations, using the models of the known two BH-domains, and a parallel search for heavy-atom derivatives are currently in progress.

This research was supported by a program project grant funded by the Public Health Service, grant number 2 PO1 Hl48807-06A1.

## References


Barrett, T., Xiao, B., Dodson, E. J., Dodson, G., Ludbrook, S. B., Nurmahomed, K., Gamblin, S. J., Musacchio, A., Smerdon, S. J. & Eccleston, J. F. (1997). *Nature (London)*, **385**, 458–461.

Boguski, M. S. & McCormick, F. (1993). *Nature (London)*, **366**, 643–654.

Bourne, H. R., Sanders, D. A. & McCormick, F. (1990). *Nature (London)*, **348**, 125–1.

Bourne, H. R., Sanders, D. A. & McCormick, F. (1991). *Nature (London)*, **349**, 117–127.

Chuang, T. H., Xu, X., Kaartinen, V., Heisterkamp, N., Groffen, J. & Bokoch, G. M. (1995). *Proc. Natl Acad. Sci. USA*, **92**, 10282–10286.

Diekmann, D., Brill, S., Garrett, M. D., Totty, N., Hsuan, J., Monfries, C., Hall, C., Lim, L. & Hall, A. (1991). *Nature (London)*, **351**, 400–402.

Hall, A. (1990). *Science*, **249**, 635–640.

Hildebrand, J. D., Taylor, J. M. & Parsons, J. T. (1996). *Mol. Cell. Biol.* **16**, 3169–3178.

Lancaster, C. A., Taylor-Harris, P. M., Self, A. J., Brill, S., van Erp, H. E. & Hall, A. (1994). *J. Biol. Chem.* **269**, 1137–1142.

Musacchio, A., Cantley, L. C. & Harrison, S. C. (1996). *Proc. Natl Acad. Sci. USA*, **93**, 14373–14378.

Otwinowski, Z. & Minor, W. (1997). *Methods Enzymol.* **273**, 307–326.

Ridley, A. J. (1994). *J. Cell Sci. (Suppl.)* **18**, 127–131.

Ridley, A. J. & Hall, A. (1992). *Cell*, **70**, 389–399.

Ridley, A. J., Paterson, H. F., Johnston, C. L., Diekmann, D. & Hall, A. (1992). *Cell*, **70**, 401–410.

Scheffzek, K., Ahmedian, M. R., Kabsch, W., Wiesmuller, L., Lautwein, A., Schmitz, F. & Wittinghofer, A. (1997). *Science*, **277**, 333–338.

Scheffzek, K., Lautwein, A., Kabsch, W., Ahmadian, M. R. & Wittinghofer, A. (1996). *Nature (London)*, **384**, 591–596.

Rittinger, K., Walker, P. A., Eccleston, J. F., Nurmahomed, K., Owen, D., Laue, E., Gamblin, S. & Smerdon, S. J. (1997). *Nature (London)*, **388**, 693–697.

Rittinger, K., Walker, P. A., Eccleston, J. F., Smerdon, S. J. & Gamblin, S. J. (1997). *Nature (London)*, **389,** 758–762.

Trahey, M., Wong, G., Halenbeck, R., Rubinfeld, B., Martin, G. A., Ladner, M., Long, C. M., Crosier, W. J., Watt, K., Koths, K. & McCormick, F. (1988). *Science*, **242**, 1697–1700.

Vogel, U. S., Dixon, R. A., Schaber, M. D., Diehl, R. E., Marshall, M. S., Scolnick, E. M., Sigal, I. S. & Gibbs, J. B. (1988). *Nature (London)*, **335**, 90–93.